Karttunen, Anssi T.; Romanoff, Jani; Reddy, J. N.

Exact microstructure-dependent Timoshenko beam element

Published in:
International Journal of Mechanical Sciences

DOI:
10.1016/j.ijmecsci.2016.03.023

Published: 01/06/2016

Document Version
Peer reviewed version

Exact microstructure-dependent Timoshenko beam element

Anssi T. Karttunen[a,b,*], Jani Romanoff[a], J.N. Reddy[b]

[a] *Aalto University, Department of Mechanical Engineering, Finland*
[b] *Texas A&M University, Department of Mechanical Engineering, USA*

Abstract

In this study, we develop an exact microstructure-dependent Timoshenko beam finite element. First, a Timoshenko beam model based on the modified couple-stress theory is reviewed briefly. The general closed-form solution to the equilibrium equations of the beam is derived. The two-dimensional in-plane stress distributions along the beam in terms of load resultants are obtained. In addition, the general solution can be used to model any distributed load which can be expressed as a Maclaurin series. Then, the solution is presented in terms of discrete finite element (FE) degrees of freedom. This representation yields the exact shape functions for the beam element. Finally, the exact beam finite element equations are obtained by writing the generalized forces at the beam ends using the FE degrees of freedom. Three calculation examples which have applications in micron systems and sandwich structures are presented.

1. Introduction

Over the past decade or two, the rise of small-scale technologies and the development of novel heterogeneous materials and periodic structures have led to a growing interest in micromechanical modeling of solids. This, in turn, has sparked interest in non-classical theories of continuum mechanics which, unlike the classical one, account for small-scale effects that may have an impact on the macro-deformation of a structure. Standard non-classical continuum theories for solids are built upon the premise that in addition to the classical force-stress vector on a plane (surface traction), a similarly defined non-vanishing *couple-stress vector* is also present. Furthermore, the stress state at a point is defined by the components of the force-stress and couple-stress tensors.

The widely used modified couple-stress theory by Yang et al. [1] provides a coherent framework for developing microstructure-dependent structural models such as beams and plates. This theory is a simplified version of the standard couple-stress theory which was conceived in the 1960s and can be obtained as a special case of, for example, a second-order rotation gradient theory or the Cosserat theory [2, 3]. An in-depth survey on the early works on the standard couple-stress theory was given by Tiersten and Bleustein [4]. The main difference between the modified couple-stress theory and the standard theory is that the couple-stress tensor is symmetric in the modified theory. This symmetry makes the strain energy independent of the antisymmetric part of the curvature tensor (the symmetric part and the couple-stress tensor are energetically conjugate) and this feature facilitates energy-based considerations. Furthermore, the modified theory contains

Recompiled, unedited accepted manuscript. **Cite as**: *Int. J. Mech. Sci.* 2016;111-112:35–42. doi link
*Corresponding author. *anssi.karttunen@iki.fi*

only one non-classical material constant in comparison to the standard theory which includes two such constants. In the modified theory, the governing equations are commonly expressed in such a form that instead of the non-classical material constant a microstructural length scale parameter appears in the equations. This parameter is typically determined either by a fit to test data or by making a reasonable choice on the basis of the topology of the microstructure at hand. In the case of the standard couple-stress theory, the task of determining the two non-classical material constants is more ambiguous.

Size-dependency is known to play a pivotal role in micro- and nano-beam structures, for examples, see the works by Lam et al. [5] and McFarland and Colton [6]. Motivated by the size-dependency, the modified couple-stress theory has been used to develop microstructure-dependent beam models. Park and Gao [7] studied the static bending of an Euler–Bernoulli beam based on the modified couple-stress theory, Kong et al. [8] established a dynamic version of such a beam, and Akgöz and Civalek [9] studied analytically the buckling problem of a microbeam. Xia et al. [10] investigated different nonlinear aspects of Euler–Bernoulli microbeams. Abdi et al. [11] and Rahaeifard et al. [12] examined small-scale electromechanical cantilever beams.

Timoshenko beam models based on the modified couple-stress theory have been formulated by Ma et al. [13], Asghari et al. [14, 15] and Reddy [16]. For further studies on microstructure-dependent Timoshenko beam models based on the modified couple-stress theory, see Refs. [17, 18, 19, 20, 21]. In addition to small-scale applications, the formulation by Reddy [16] has recently been used to study macroscale web-core sandwich beams by Romanoff et al. [22, 23].

Finite element models for Timoshenko beams based on the modified couple-stress theory have been presented by Arbind and Reddy [24], Komijani et al. [25] and Kahrobaiyan et al. [26]. In developing their Timoshenko beam element, Kahrobaiyan et al. [26] assumed the microstructural length scale parameter to be very small in comparison to the beam length. Such an assumption is not valid, for example, in the study of web-core sandwich beams where the value of the length scale parameter may be up to one-fourth of the total beam length (see, Romanoff and Reddy [22]). In other words, the length scale parameter is not small in comparison to the total length of a web-core beam and, thus, the governing equations should not be simplified in the same way as in Ref. [26]. We also note that Arbind and Reddy [24] and Komijani et al. [25] used approximate polynomial interpolation functions in their finite element formulations. In light of the foregoing, the main objective of this study is to formulate an exact, linearly elastic microstructure-dependent Timoshenko beam element without making any numerical approximations or simplifying assumptions in the course of the development. The element is essentially an alternative form of the general closed-form solution to the linearized governing equations of the modified couple-stress Timoshenko beam model by Reddy [16]. As an additional novelty, the general solution to be developed in this paper can be used to model any distributed load which can be expressed as a Maclaurin series.

In more detail, the rest of the paper is organized in the following way. In Section 2, the microstructure-dependent Timoshenko beam model is reviewed briefly. The general solution to the governing equations of the model is developed by taking use of a change of variables similar to that employed by Asghari et al. [15]. The homogeneous solution consists of polynomial and hyperbolic functions and includes six constant coefficients. In Section 3, these constants are expressed in terms of six discrete nodal degrees of freedom defined at the ends of the beam. This representation enables the formulation of the exact beam finite element. In Section 4, case studies considering beams with microstructures are presented. Conclusions are drawn in Section 5.

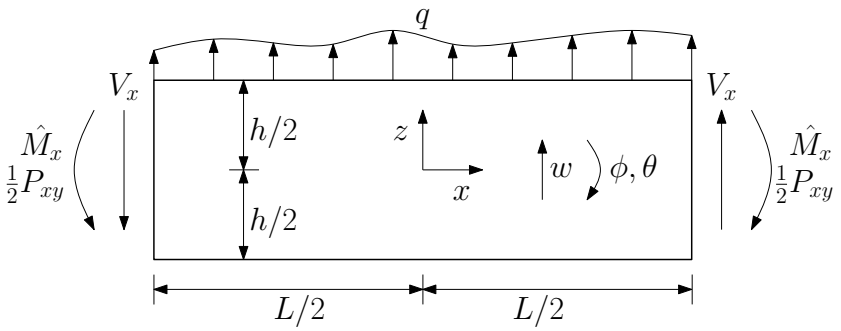

Figure 1: Microstructure-dependent Timoshenko beam subjected to a distributed load $q(x)$. The positive directions of the kinematic variables and the generalized forces at the beam ends are shown.

2. Couple-stress Timoshenko beam

2.1. Governing equations

Let us consider the microstructure-dependent Timoshenko beam presented in Fig. 1. Following Reddy [16], the beam has a rectangular cross-section of constant thickness t and the length and height of the beam are L and h, respectively. The displacement field of the beam can be written as

$$U_x(x,z) = z\phi(x) \ , \quad U_z(x,z) = w(x) \ , \tag{1}$$

where ϕ is the rotation of the cross-section at the central axis of the beam and w is the transverse deflection of the central axis. The axial normal strain, transverse shear strain and the only non-zero component of the curvature tensor are

$$\begin{aligned} \epsilon_x &= \frac{\partial U_x}{\partial x} = z\frac{\partial \phi}{\partial x} \ , \quad \gamma_{xz} = \frac{\partial U_x}{\partial z} + \frac{\partial U_z}{\partial x} = \phi + \frac{\partial w}{\partial x} \ , \\ \chi_{xy} &= \frac{1}{2}\frac{\partial \omega_y}{\partial x} = \frac{1}{4}\frac{\partial}{\partial x}\left(\frac{\partial U_x}{\partial z} - \frac{\partial U_z}{\partial x}\right) = \frac{1}{4}\left(\frac{\partial \phi}{\partial x} - \frac{\partial^2 w}{\partial x^2}\right) \ , \end{aligned} \tag{2}$$

respectively. In the last of the previous equations, ω_y is the only nonzero component of the rotation vector. The axial normal stress, transverse shear stress and the couple-stress are obtained from the constitutive relations

$$\sigma_x = E(z)\epsilon_x \ , \quad \tau_{xz} = G(z)\gamma_{xz} \ , \quad m_{xy} = \mathbf{2}G(z)l^2\chi_{xy} \ , \tag{3}$$

respectively, where $E(z)$ and $G(z)$ are the Young's modulus and shear modulus, respectively, and l is the microstructural length scale parameter. The equilibrium equations for the beam subjected to a distributed load $q(x)$ read [13, 16]

$$\frac{\partial Q_x}{\partial x} + \frac{1}{2}\frac{\partial^2 P_{xy}}{\partial x^2} = -q \ , \tag{4}$$

$$Q_x - \frac{\partial M_x}{\partial x} - \frac{1}{2}\frac{\partial P_{xy}}{\partial x} = 0 \ . \tag{5}$$

Above, the load resultants, which act at an arbitrary cross-section of the beam, are defined as [16]

$$Q_x = \int_A \tau_{xz} dA = D_Q \left(\phi + \frac{\partial w}{\partial x} \right) \ , \tag{6}$$

$$P_{xy} = \int_A m_{xy} dA = \frac{1}{2} S_{xy} \left(\frac{\partial \phi}{\partial x} - \frac{\partial^2 w}{\partial x^2} \right) \ , \tag{7}$$

$$M_x = \int_A z \sigma_x dA = D_{xx} \frac{\partial \phi}{\partial x} \ , \tag{8}$$

where we have $D_Q = K_s S_{xz}$ with the Timoshenko shear coefficient K_s, and D_{xx}, S_{xz} and S_{xy} are the bending, transverse shear, and in-plane shear stiffness coefficients, respectively. These stiffness coefficients may be determined, for example, according to an isotropic material [13]; two-constituent functionally graded material [16] or according to sandwich beam theory [22]. By writing the equilibrium equations (4) and (5) in terms of the kinematic variables, we obtain

$$D_Q \left(\phi' + w'' \right) + \frac{1}{4} S_{xy} \left(\phi''' - w'''' \right) = -q \ , \tag{9}$$

$$D_Q \left(\phi + w' \right) - D_{xx} \phi'' - \frac{1}{4} S_{xy} \left(\phi'' - w''' \right) = 0 \ , \tag{10}$$

where prime denotes differentiation with respect to x. As for the boundary conditions, one element in each of the following pairs should be specified at $x = \pm L/2$

$$V_x \quad \text{or} \quad w \ , \tag{11}$$

$$\hat{M}_x \quad \text{or} \quad \phi \ , \tag{12}$$

$$\frac{1}{2} P_{xy} \quad \text{or} \quad \theta \equiv -\frac{\partial w}{\partial x} \ , \tag{13}$$

where $\theta(x)$ is the slope at the central axis of the beam and

$$\hat{M}_x = M_x + \frac{1}{2} P_{xy} \ , \quad V_x = Q_x + \frac{1}{2} \frac{\partial P_{xy}}{\partial x} \ . \tag{14}$$

The equilibrium equations (9) and (10) can be rendered amenable to an analytical solution by introducing the variables [15]

$$\gamma \equiv \gamma_{xz} = \phi + w' \quad \text{and} \quad \omega \equiv 2\omega_y = \phi - w' \ . \tag{15}$$

Now we can write Eqs. (9) and (10) in the form

$$D_Q \gamma' + \frac{1}{4} S_{xy} \omega''' = -q \ , \tag{16}$$

$$D_Q \gamma - \frac{D_{xx}}{2} \gamma'' = \left(\frac{D_{xx}}{2} + \frac{S_{xy}}{4} \right) \omega'' \ . \tag{17}$$

In summary, after obtaining a solution to Eqs. (16) and (17), the original kinematic variables $\phi = (\gamma + \omega)/2$ and $w' = (\gamma - \omega)/2$ are retrieved from Eqs. (15). Next we consider the homogeneous and particular solutions which provide the general solution

$$w = w_h + w_p \ , \quad \phi = \phi_h + \phi_p \tag{18}$$

to the equilibrium equations (9) and (10).

2.2. Homogeneous solution

In the case of the homogeneous solution, that is, for $q(x) = 0$, we obtain

$$w_h = C_1 + C_2 A_2 + C_3 A_3 + C_4 A_4 + C_5 A_5 + C_6 A_6 \ , \tag{19}$$

$$\begin{aligned}\phi_h = &-C_2 \frac{\partial A_2}{\partial x} - C_3 \frac{\partial A_3}{\partial x} + C_4 \left[\frac{D_{xx} S_{xy} \sinh\left(\frac{2\alpha x}{\beta}\right)}{2\beta} - \frac{\partial A_4}{\partial x} \right] \\ &- C_5 \left[\frac{S_{xy}(2D_{xx} + S_{xy}) \sinh^2\left(\frac{\alpha x}{\beta}\right)}{4 D_Q (D_{xx} + S_{xy})} + \frac{\partial A_5}{\partial x} \right] \\ &+ C_6 \left[\frac{2D_{xx} + S_{xy} + S_{xy} \cosh\left(\frac{2\alpha x}{\beta}\right)}{2(D_{xx} + S_{xy})} - \frac{\partial A_6}{\partial x} \right] \ ,\end{aligned} \tag{20}$$

where

$$\alpha = D_Q \left(D_{xx} + S_{xy} \right) \ , \tag{21}$$

$$\beta = \sqrt{D_Q D_{xx} S_{xy} \left(D_{xx} + S_{xy} \right)} \tag{22}$$

and

$$\begin{aligned}A_2(x) &= -\frac{x}{2} \ , \quad A_3(x) = -\frac{x^2}{4} \ , \\ A_4(x) &= D_{xx} \frac{S_{xy}(2D_{xx} + S_{xy}) \cosh\left(\frac{2\alpha x}{\beta}\right) - 2\alpha x^2}{8\alpha(D_{xx} + S_{xy})} \ , \\ A_5(x) &= S_{xy} \frac{2\alpha x \left[3(2D_{xx} + S_{xy})^2 - 2\alpha x^2\right] - 3\beta(2D_{xx} + S_{xy})^2 \sinh\left(\frac{2\alpha x}{\beta}\right)}{96\alpha^2(D_{xx} + S_{xy})} \ , \\ A_6(x) &= \frac{\alpha x \left[3(2D_{xx} + S_{xy})^2 + 3S_{xy}^2 - 4\alpha x^2\right] + 3S_{xy}\beta(2D_{xx} + S_{xy}) \sinh\left(\frac{2\alpha x}{\beta}\right)}{24\alpha(D_{xx} + S_{xy})^2} \ .\end{aligned} \tag{23}$$

We see from Eqs. (19)–(23) that the relation $\phi_h' = -w_h''$ ($\phi_h' = \theta_h'$), which holds for the classical Timoshenko beam, does not hold in the present case due to the hyperbolic terms in the solution. Note that the constant C_1 corresponds to rigid body translation in the $z-$direction and C_2 to a rigid body rotation about the $y-$axis. We calculate the load resultants (6)–(8) and $(14)_2$ using the stresses (3) and the homogeneous solution (19) and (20). Then we can express the constants C_3, C_4, C_5 and C_6 in terms of the load resultants and substitute them back into the stresses (3) to obtain the general 2D stress distributions

$$\sigma_x(x,z) = \frac{E(z) M_x(x) z}{D_{xx}} \ , \tag{24}$$

$$\tau_{xz}(x,z) = \frac{G(z) Q_x(x)}{D_Q} \ , \tag{25}$$

$$m_{xy}(x,z) = \frac{G(z) P_{xy}(x) l^2}{S_{xy}} \ . \tag{26}$$

We note already at this point that even if the particular solution for a distributed load developed in the next section is included in the general solution, the expressions (24)–(26) remain the same.

2.3. Particular solution

To obtain a solution for a distributed load which is of general nature, we consider the load to be of the form

$$q(x) = q_n x^n \ . \tag{27}$$

Accordingly, we write

$$w_p \to w_p^n \qquad \text{and} \qquad \phi_p \to \phi_p^n \ . \tag{28}$$

The particular solution is then

$$\begin{aligned} w_p^n = {} & \frac{q_n x^{2+n}}{4(D_{xx}+S_{xy})(1+n)(2+n)} \left[\frac{4x^2}{(3+n)(4+n)} - D_{xx}(2D_{xx}+S_{xy}) \frac{S_{xy}(D_{xx}+S_{xy})\alpha+\beta^2}{\alpha\beta^2} \right] \\ & - q_n x^n \frac{2^{-5-n} D_{xx}(2D_{xx}+S_{xy}) \left(D_{xx} S_{xy}^2 (D_{xx}+S_{xy})\alpha^2 + \beta^4 \right)}{(D_{xx}+S_{xy})\alpha^3\beta^2} \\ & \times \left[\left(\frac{\alpha x}{\beta} \right)^n \Gamma^- + e^{\frac{4\alpha x}{\beta}} \left(-\frac{\alpha x}{\beta} \right)^n \Gamma^+ \right] e^{-\frac{2\alpha x}{\beta}} \left(-\frac{\alpha x^2}{D_{xx} S_{xy}} \right)^{-n} \ , \end{aligned} \tag{29}$$

$$\begin{aligned} \phi_p^n = {} & -\frac{q_n x^{1+n}}{4(D_{xx}+S_{xy})(1+n)} \left[\frac{4x^2}{(2+n)(3+n)} + D_{xx}(2D_{xx}+S_{xy}) \frac{S_{xy}(D_{xx}+S_{xy})\alpha-\beta^2}{\alpha\beta^2} \right] \\ & + q_n x^n \frac{2^{-4-n} D_{xx}(2D_{xx}+S_{xy}) \left(D_{xx} S_{xy}^2 (D_{xx}+S_{xy})\alpha^2 - \beta^4 \right)}{(D_{xx}+S_{xy})\alpha^2\beta^3} \\ & \times \left[\left(\frac{\alpha x}{\beta} \right)^n \Gamma^- - e^{\frac{4\alpha x}{\beta}} \left(-\frac{\alpha x}{\beta} \right)^n \Gamma^+ \right] e^{-\frac{2\alpha x}{\beta}} \left(-\frac{\alpha x^2}{D_{xx} S_{xy}} \right)^{-n} \ , \end{aligned} \tag{30}$$

where the incomplete gamma functions can be written as [27]

$$\Gamma^{\mp} = \Gamma\left(n+1, \mp\frac{2\alpha x}{\beta} \right) = n! e^{\pm\frac{2\alpha x}{\beta}} \sum_{m=0}^{n} \frac{\left(\mp\frac{2\alpha x}{\beta} \right)^m}{m!} \qquad \text{for} \qquad n = 0, 1, 2, \ldots \tag{31}$$

As an elementary example, we consider a uniformly distributed load (i.e. $n = 0$ and $q_n = q_0$) and Eqs. (29)–(31) yield

$$w_p^0 = q_0 \frac{2D_Q^2 x^4 (D_{xx}+S_{xy})^2 - 6D_Q x^2 (D_{xx}+S_{xy})(2D_{xx}+S_{xy})^2 - 3D_{xx}S_{xy}(2D_{xx}+S_{xy})^2}{48 D_Q^2 (D_{xx}+S_{xy})^3} \ , \tag{32}$$

$$\phi_p^0 = -q_0 x \frac{2D_Q x^2 (D_{xx}+S_{xy}) + 3S_{xy}(2D_{xx}+S_{xy})}{12 D_Q (D_{xx}+S_{xy})^2} \ . \tag{33}$$

Due to the linearity of the problem, the particular solution by Eqs. (29) and (30) is valid for any distributed load which can be expressed as a Maclaurin series

$$q(x) = q(0) + \frac{q'(0)}{1!}x + \frac{q''(0)}{2!}x^2 + \frac{q'''(0)}{3!}x^3 + \ldots = \sum_{n=0}^{\infty} q_n x^n \ . \tag{34}$$

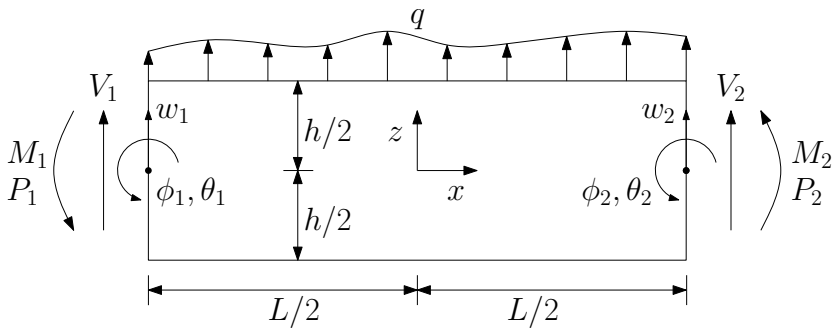

Figure 2: Set–up according to which the exact microstructure-dependent Timoshenko beam element based on the modified couple-stress theory is developed.

3. Exact microstructure-dependent beam element

The general solution (18) can be used as the basis for the formulation of an exact microstructure-dependent Timoshenko beam finite element. The element is obtained by presenting the general solution in terms of discrete degrees of freedom. For reference, a similar finite element formulation for a classical isotropic beam based on an exact elasticity solution has been presented by Karttunen and von Hertzen [28].

3.1. General solution in terms of FE-degrees of freedom

Fig. 2 presents the setting according to which the element is developed. Both nodes in Fig. 2 have three degrees of freedom. For nodes $i = 1, 2$, we have transverse displacements w_i and rotations ϕ_i and θ_i. In the classical case, there is only one rotation [29]. Using the solution (18), we obtain for nodes 1 and 2 the following six equations

$$\begin{aligned} w_1 &= w(-L/2) \ , & w_2 &= w(L/2) \ , \\ \phi_1 &= -\phi(-L/2) \ , & \phi_2 &= -\phi(L/2) \ , \\ \theta_1 &= -\theta(-L/2) \ , & \theta_2 &= -\theta(L/2) \ . \end{aligned} \tag{35}$$

We can solve the six unknown constants C_j $(j = 1, \ldots, 6)$ from Eqs. (35). The lengthy explicit expressions for these are given in Appendix A. By substituting the solved constants into Eqs. (18), we can write the transverse deflection and the rotation of the cross-section in the form

$$w(x) = \mathbf{N}_w \mathbf{u} + w^q \ , \tag{36}$$

$$\phi(x) = \mathbf{N}_\phi \mathbf{u} + \phi^q \ , \tag{37}$$

where

$$\mathbf{u} = \{w_1 \quad \phi_1 \quad \theta_1 \quad w_2 \quad \phi_2 \quad \theta_2\}^{\mathrm{T}} \tag{38}$$

is the displacement vector and $\mathbf{N}_w$ and $\mathbf{N}_\phi$ are the shape functions. Functions $w^q(x)$ and $\phi^q(x)$ depend on the particular distributed load at hand. By looking at the general solution (18)–(20) and the constants provided in Appendix A, we see that the shape functions contain hyperbolic terms in addition to mere polynomials that suffice in the classical case. We note that the shape functions as such are not used in the current developments, that is, the solution along a beam element is obtained by substituting constants C_j $(j = 1, \ldots, 6)$ and the nodal displacements into the general solution (18). After this the calculation of the 2D displacements (1), strains (2), and stresses (3) is straightforward.

3.2. Finite element equations

To obtain the finite element equations, we substitute constants C_3, C_4, C_5 and C_6 into Eqs. (13) and (14) to calculate the generalized forces at nodes $i = 1, 2$, with the notion that the positive directions are taken to be according to Fig. 1 so that

$$\begin{aligned} V_1 &= -V_x(-L/2) \ , & V_2 &= V_x(L/2) \ , \\ M_1 &= \hat{M}_x(-L/2) \ , & M_2 &= -\hat{M}_x(L/2) \ , \\ P_1 &= (1/2)P_{xy}(-L/2) \ , & P_2 &= -(1/2)P_{xy}(L/2) \ . \end{aligned} \tag{39}$$

The conventional presentation for the 1D beam element is obtained by writing Eqs. (39) in the form

$$\mathbf{K}\mathbf{u} = \mathbf{f} + \mathbf{q} \ , \tag{40}$$

where $\mathbf{K}$ is the stiffness matrix (see Appendix B), $\mathbf{q}$ is the force vector related to the distributed load and

$$\mathbf{f} = \{V_1 \quad M_1 \quad P_1 \quad V_2 \quad M_2 \quad P_2\}^{\mathrm{T}} \tag{41}$$

is the nodal force vector.

4. Case studies

In this section we study three calculation examples. Fig. 3(a) shows an end-loaded cantilever beam, which is a common component in micro- and nanoelectromechanical systems. The relative differences between the classical and couple-stress solutions are studied at the loaded end. In Fig. 3(b), three-point bending is modeled by a symmetric half of a simply-supported web-core sandwich beam. The number of unit cells along the beam is varied in the calculations. A web-core sandwich beam that consists of four unit cells is presented in Fig. 3(c). In this case, the computations are carried out using four beam elements. Note that if the sandwich beams were to be modeled in 3D, there would be no need to account for the couple-stresses. However, when using a 1D beam model, it is beneficial to employ the modified couple-stress theory. A unit cell of a web-core sandwich beam constitutes a microstructural building block and the length scale parameter l is taken equal to the length of the unit cell. For more details, see the works by Romanoff et al. [22, 23].

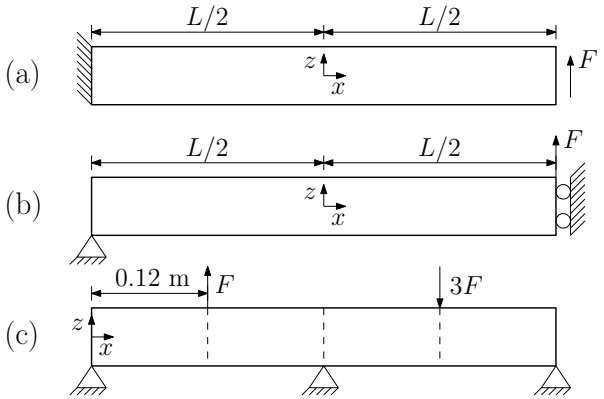

Figure 3: a) End-loaded cantilever beam. b) Three-point bending of a web-core sandwich beam modeled by a symmetric half. c) Web-core sandwich beam which consists of four unit cells.

4.1. End-loaded cantilever

The solution to the cantilever problem in Fig. 3(a) is obtained using one beam element and by applying the boundary conditions $w_1 = \phi_1 = \theta_1 = 0$. The transverse deflection $w(x)$ and rotation $\phi(x)$ are then obtained from Eqs. (36) and (37). Alternatively, using the general solution (18), the six boundary conditions read

$$\begin{aligned} &x = -L/2: \;\; w = \phi = \theta = 0 \;, \\ &x = +L/2: \;\; \hat{M}_x = P_{xy} = 0 \;, \;\; V_x = F \;. \end{aligned} \tag{42}$$

The transverse deflection is

$$\begin{aligned} w(x) = &\frac{F(L+2x)\left[6(2D_{xx}+S_{xy})^2 + \alpha(5L-2x)(L+2x)\right]}{48\alpha(D_{xx}+S_{xy})} \\ &- \frac{F\beta(2D_{xx}+S_{xy})^2 \mathrm{sech}\left(\frac{2\alpha L}{\beta}\right)\left[\sinh\left(\frac{2\alpha L}{\beta}\right) - \sinh\left(\frac{\alpha(L-2x)}{\beta}\right)\right]}{8\alpha^2(D_{xx}+S_{xy})} \;. \end{aligned} \tag{43}$$

The classical solution is obtained by setting the hyperbolic terms and S_{xy} to zero. The relative difference between the classical and couple-stress solutions is given by

$$w_{\mathrm{rel}} = 100 \times (w_{\mathrm{clas}} - w_{\mathrm{couple}})/w_{\mathrm{couple}} \;. \tag{44}$$

Let us consider an isotropic homogeneous beam so that $D_{xx} = EI$, $D_Q = K_s GA$, $S_{xy} = GAl^2$ where $I = th^3/12$ is the second moment of area and $A = ht$ is the cross-sectional area. We choose the parameter values $E = 1$, $h = 1$, $t = h$, $L = 10h$, $F = 1$ and $K_s = 5/6$. The relative difference (44) at $x = L/2$ as a function of the ratio l/h for three different values of the Poisson ratio ν is shown in Fig. 4. We observe two trends from the figure. First, at low $l/h-$ratios, the relative difference between the solutions is insignificant, for example, at $l/h = 0.1$, we have $w_{\mathrm{rel}} = 4\%$ for $\nu = 0.5$. However, at $l/h = 0.5$ the difference is already 100% due to the exponential nature of the curve. Second, the relative difference increases for decreasing values of the Poisson ratio.

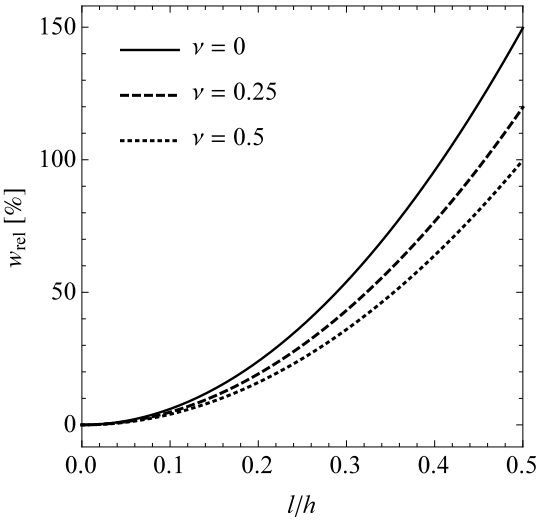

Figure 4: Relative difference between the classical and couple-stress solutions at the loaded end of a cantilever beam.

4.2. Three-point bending of a sandwich beam

Similarly to the previous problem the solution to the three-point bending by a symmetric half is obtained using one element. The boundary conditions are $w_1 = \phi_2 = \theta_2 = 0$. By employing the the general solution directly, the six boundary conditions are

$$\begin{aligned} x = -L/2: \;& w = \hat{M}_x = P_{xy} = 0 \;, \\ x = +L/2: \;& \phi = \theta = 0 \;,\; V_x = F \;. \end{aligned} \tag{45}$$

The transverse deflection is

$$\begin{aligned} w(x) = & \frac{F(L+2x)\left[6(2D_{xx}+S_{xy})^2 + \alpha\left(11L^2 - 4Lx - 4x^2\right)\right]}{48\alpha(D_{xx}+S_{xy})} \\ & - \frac{F(\beta D_{xx} S_{xy})^2 (2D_{xx}+S_{xy})^2 \operatorname{sech}\left(\frac{2\alpha L}{\beta}\right) \sinh\left(\frac{\alpha(L+2x)}{\beta}\right)}{8(D_{xx}+S_{xy})\left(\beta \times \beta\right)^{5/2}} \;. \end{aligned} \tag{46}$$

The classical solution is obtained by setting the hyperbolic terms and S_{xy} to zero. For a web-core sandwich beam, we take $D_{xx} = 657$ kNm, $D_Q = 388$ kN/m and $S_{xy} = 4.33$ kNm according to Romanoff and Reddy [22]. The load is $F = 1$ kN/m and the length of one unit cell is 0.12 m. Fig. 5(a) shows the relative difference between the classical and couple-stress solutions as a function of the number of the unit cells along the beam at three points. The differences are significant for low numbers of unit cells, that is, for high $l/L-$ratios. Fig. 5(b) presents the load resultants along the beam in the case of two unit cells. The straight line $\hat{M}_x + (1/2)P_{xy}$ corresponds to the moment M_x of the classical solution.

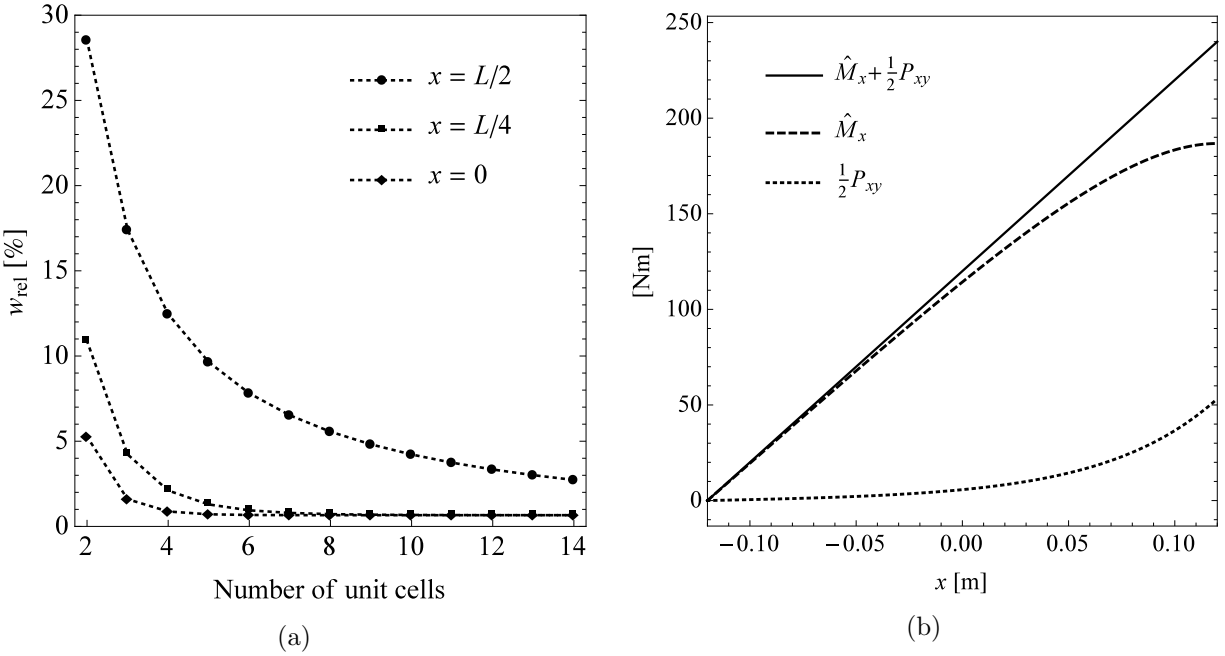

Figure 5: a) Relative difference between the classical and couple-stress solutions. b) Load resultant distributions.

4.3. Sandwich beam on three supports

Finally, we study the web-core sandwich beam shown in Fig. 3(c) which consists of four unit cells. The parameter values are the same as in the previous example, with the exception that now $F = 10$ kN/m. The beam is modeled using four finite elements. Fig. 6 shows the transverse deflection along the beam according to classical and couple-stress solutions. A brief derivation for the classical Timoshenko beam element applicable to the present case can be found in Appendix C. It has been shown by Romanoff et al. [22, 23] that couple-stress based solutions for web-core sandwich beams are in very good agreement with experimental results and with the 'Allen solutions' unlike classical Timoshenko beam solutions when the beam has only a few unit cells. In the present case, we see from Fig. 6 that the maximum deflection of the classical beam is nearly double that of the couple-stress beam. In addition, the zigzag-type deflection shape given by the classical Timoshenko beam is not physically plausible.

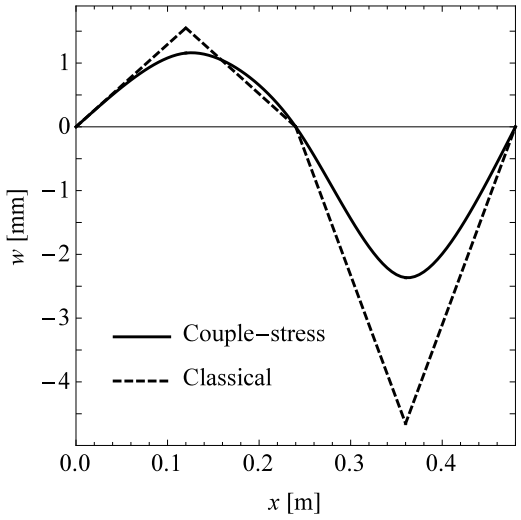

Figure 6: Transverse deflection of a web-core sandwich beam according to classical and couple-stress based solutions.

5. Conclusions

In this paper, we formulated an exact beam finite element which is an alternative representation of the general closed-form solution to the equilibrium equations of a couple-stress based Timoshenko beam model. The element has six degrees of freedom, namely deflection and two rotations at each of its two nodes. It is easy to use the beam element to model frames and beams resting on multiple supports and, thus, it essentially extends the applicability of the general closed-form solution.

In general, it is straightforward to derive analytical closed-form solutions for linear beam models and develop finite elements using these solutions. By following the methodology presented in this paper, all numerical locking problems are avoided in finite element computations. Shape functions obtained via analytical solutions may also be used as first approximations in refined finite element formulations which include, for example, the non-linear von Kármán strains. Furthermore, the analytical solutions can be used to develop consistent mass and geometric stiffness matrices. Such extensions would enable one to study, for example, the linear vibrations of an initially prestressed microstructure-dependent beam.

Appendix A. Finite element related constants

Explicit expressions for constants C_j $(j = 1, \ldots, 6)$ solved from Eqs. (35) read

$$C_1 = \frac{w_1 + w_2}{2} + \zeta \left[\beta L - 2D_{xx}S_{xy}\frac{\hat{c}}{\hat{s}}\right] \frac{\phi_1 - \phi_2}{16\beta(D_{xx} + S_{xy})} + S_{xy}\left[\beta L + 2\zeta D_{xx}\frac{\hat{c}}{\hat{s}}\right] \frac{\theta_1 - \theta_2}{16\beta(D_{xx} + S_{xy})} , \tag{A.1}$$

$$\begin{aligned} C_2 = {} & \left[6D_{xx}\alpha\zeta - 3\alpha(4D_{xx}^2 + D_Q D_{xx}L^2 + 2D_{xx}S_{xy} + D_Q S_{xy}L^2)\hat{c}\right] \frac{w_2 - w_1}{\eta} \\ & + \left\{\zeta\left[\alpha L(D_Q L^2 - 12D_{xx} - 6S_{xy})\hat{c} + 3\beta(4D_{xx} - D_Q L^2 + 2S_{xy})\hat{s}\right] + 2\alpha L^3 D_Q D_{xx}\right\} \frac{\phi_1 + \phi_2}{4\eta} \\ & + \left[(D_Q L^2 - 12D_{xx} - 6S_{xy})\alpha L S_{xy}\hat{c} - 2\alpha L D_{xx}(12D_{xx} + D_Q L^2 + 6S_{xy})\right. \\ & \left. + 3\beta\zeta(4D_{xx} + D_Q L^2 + 2S_{xy})\hat{c}\right] \frac{\theta_1 + \theta_2}{4\eta} , \end{aligned} \tag{A.2}$$

$$C_3 = \left[\zeta\beta - \alpha L D_{xx}(1/\hat{s})\right] \frac{\phi_1 - \phi_2}{\beta L(D_{xx} + S_{xy})} + \left[\beta S_{xy} + \alpha L D_{xx}(1/\hat{s})\right] \frac{\theta_1 - \theta_2}{\beta L(D_{xx} + S_{xy})} , \tag{A.3}$$

$$C_4 = \frac{\alpha}{\beta\hat{s}}(\phi_1 - \phi_2 - \theta_1 + \theta_2) , \tag{A.4}$$

$$\begin{aligned} C_5 = {} & 24\alpha^2\left[\zeta + S_{xy}\hat{c}\right] \frac{w_2 - w_1}{S_{xy}\eta} + 2D_Q\left[\alpha^2 L^3 + 3\zeta S_{xy}\left(\beta\hat{s} - \alpha L\hat{c}\right)\right] \frac{\phi_1 + \phi_2}{S_{xy}\eta} \\ & - \left\{2\alpha L D_Q\left[6\zeta(D_{xx} + S_{xy}) + \alpha L^2 + 3S_{xy}^2\hat{c}\right] + 6\zeta\beta D_Q S_{xy}\hat{s}\right\} \frac{\theta_1 + \theta_2}{S_{xy}\eta} , \end{aligned} \tag{A.5}$$

$$\begin{aligned} C_6 = {} & \left[12\alpha\zeta(D_{xx} + S_{xy})\hat{s}^2\right] \frac{w_2 - w_1}{\eta} + \left\{3\zeta^2\left[\beta\hat{s} - \alpha L\hat{c}\right] - \alpha^2 L^3\right\} \frac{\phi_1 + \phi_2}{2\eta} \\ & + \left\{\alpha L\left[6\zeta(D_{xx} + S_{xy}) + \alpha L^2\right] - 3\alpha L\zeta S_{xy}\hat{c} - 3\beta\zeta^2\hat{s}\right\} \frac{\theta_1 + \theta_2}{2\eta} , \end{aligned} \tag{A.6}$$

where α and β are given by Eqs. (21) and (22), respectively, and

$$\zeta = 2D_{xx} + S_{xy} \ , \ \hat{c} = \cosh\left(\frac{\alpha L}{\beta}\right) \ , \ \hat{s} = \sinh\left(\frac{\alpha L}{\beta}\right) \tag{A.7}$$

$$\eta = \alpha L\left[3\zeta^2 + \alpha L^2\right]\cosh\left(\frac{\alpha L}{\beta}\right) - 3\beta\zeta^2\sinh\left(\frac{\alpha L}{\beta}\right) . \tag{A.8}$$

Appendix B. Microstructure-dependent stiffness matrix

$$\mathbf{K} = \begin{bmatrix} K_{11} & & S & & & \\ K_{21} & K_{22} & & Y & & \\ K_{31} & K_{32} & K_{33} & & M. & \\ K_{41} & K_{42} & K_{43} & K_{44} & & \\ K_{51} & K_{52} & K_{53} & K_{54} & K_{55} & \\ K_{61} & K_{62} & K_{63} & K_{64} & K_{65} & K_{66} \end{bmatrix} \tag{B.1}$$

The coefficients of the stiffness matrix (B.1) can be written as

$$K_{11} = \frac{12\alpha^2\hat{c}}{\eta}\left(D_{xx} + S_{xy}\right) \ , \tag{B.2}$$

$$K_{21} = \frac{3\alpha^2\zeta}{\beta\eta}\left(\beta L\hat{c} - D_{xx}S_{xy}\hat{s}\right) \ , \tag{B.3}$$

$$K_{31} = \frac{3\alpha\beta}{D_{xx}\eta}\left(\beta L\hat{c} + D_{xx}\zeta\hat{s}\right) \ , \tag{B.4}$$

$$\begin{aligned} K_{22} = \frac{D_Q}{4\beta L\eta}\Bigg[&\beta L\zeta^2\left(3\zeta^2 + 4\alpha L^2 - 3D_{xx}S_{xy}\right)\hat{c} \\ &+ \alpha L^2 D_{xx}S_{xy}\left(3\zeta^2 + \alpha L^2\cosh\left(\frac{2\alpha L}{\beta}\right)\right)\frac{1}{\hat{s}} - 3D_{xx}S_{xy}\zeta^4\hat{s}\Bigg] \ , \end{aligned} \tag{B.5}$$

$$\begin{aligned} K_{32} = -\frac{D_Q S_{xy}}{4\beta L\eta}\Bigg[&L\left(\alpha L D_{xx}\left(\alpha L^2 + 3\zeta^2\right)\frac{\hat{c}}{\hat{s}} - \beta\zeta\left(3\zeta\left(3D_{xx} + S_{xy}\right) + 4\alpha L^2\right)\right)\hat{c} \\ &+ D_{xx}\left(\alpha^2 L^4 + 3\alpha L^2\zeta S_{xy} + 3\zeta^3 S_{xy}\right)\hat{s}\Bigg] \ , \end{aligned} \tag{B.6}$$

$$\begin{aligned} K_{52} = \frac{D_Q}{4L\beta\eta}\Bigg[&3\zeta^4 D_{xx}S_{xy}\hat{s} + L\beta\zeta^2\left(3D_{xx}S_{xy} + 2L^2\alpha - 3\zeta^2\right)\hat{c} \\ &- \frac{\alpha L^2 D_{xx}S_{xy}}{\hat{s}}\left(3\zeta^2\left(\hat{c}^2 + \hat{s}^2\right) + \alpha L^2\right)\Bigg] \ , \end{aligned} \tag{B.7}$$

$$\begin{aligned} K_{62} = -\frac{D_Q S_{xy}}{4L\beta\eta}\Bigg[&D_{xx}\left(\alpha^2 L^4 + 3(\alpha L^2\zeta - \zeta^3)S_{xy}\right)\hat{s} \\ &+ L\left(\beta\zeta(9\zeta D_{xx} + 3\zeta S_{xy} - 2\alpha L^2) - \alpha L D_{xx}\left(\alpha L^2 + 3\zeta^2\right)\frac{\hat{c}}{\hat{s}}\right)\hat{c}\Bigg] \ , \end{aligned} \tag{B.8}$$

$$\begin{aligned} K_{33} = \frac{D_Q S_{xy}}{4L\beta\eta}\Bigg[&L\left(\beta(4\alpha L^2 S_{xy} - 3\zeta^2(D_{xx} - S_{xy})) + \alpha L D_{xx}(\alpha L^2 + 3\zeta^2)\frac{\hat{c}}{\hat{s}}\right)\hat{c} \\ &+ D_{xx}(\alpha^2 L^4 - 3\zeta^2 S_{xy}^2 + 3\alpha L^2\zeta(2D_{xx} + 3S_{xy}))\hat{s}\Bigg] \ , \end{aligned} \tag{B.9}$$

$$\begin{aligned} K_{63} = \frac{D_Q S_{xy}}{4L\beta\eta}\Bigg[&L\left(\beta(3\zeta^2(D_{xx} - S_{xy}) + 2\alpha L^2 S_{xy}) - \alpha L D_{xx}(\alpha L^2 + 3\zeta^2)\frac{\hat{c}}{\hat{s}}\right)\hat{c} \\ &+ D_{xx}(\alpha^2 L^4 + 3\zeta^2 S_{xy}^2 + 3\alpha L^2\zeta(2D_{xx} + 3S_{xy}))\hat{s}\Bigg] \end{aligned} \tag{B.10}$$

$$\begin{aligned} &K_{41} = -K_{11} \ , \quad K_{51} = K_{21} \ , \quad K_{61} = K_{31} \ , \\ &K_{42} = -K_{21} \ , \quad K_{43} = -K_{31} \ , \quad K_{53} = K_{62} \ , \\ &K_{44} = K_{11} \ , \quad K_{54} = -K_{21} \ , \quad K_{64} = -K_{31} \ , \\ &K_{55} = K_{22} \ , \quad K_{65} = K_{32} \ , \quad K_{66} = K_{33} \end{aligned} \tag{B.11}$$

See Eqs. (21) and (22) for α and β, respectively, and Eqs. (A.7) and (A.8) for ζ, η, $\hat{c}$ and $\hat{s}$.

Appendix C. Classical Timoshenko beam element

The equilibrium equations of the classical Timoshenko beam are obtained by setting $S_{xy} = 0$ in Eqs. (9) and (10). In the absence of the distributed load, the general solution to the obtained equations is

$$w(x) = \frac{D_{xx}\left(6c_3 + 6c_1 x - 3c_2 x^2\right) - D_Q x^3 (c_1 + c_4)}{6D_{xx}} \ , \tag{C.1}$$

$$\phi(x) = \frac{2D_{xx}(c_2 x + c_4) + D_Q x^2 (c_1 + c_4)}{2D_{xx}} \ . \tag{C.2}$$

Similarly to the developments in Section 3, the element has two nodes, each of which has two degrees of freedom. For nodes $i = 1, 2$, we have transverse displacements w_i and rotations ϕ_i. Using the solution above, we obtain for nodes 1 and 2 the following four equations

$$\begin{aligned} w_1 &= w(-L/2) \ , & w_2 &= w(L/2) \ , \\ \phi_1 &= -\phi(-L/2) \ , & \phi_2 &= -\phi(L/2) \ . \end{aligned} \tag{C.3}$$

We can solve the four unknown constants c_j $(j = 1, \ldots, 4)$ from Eqs. (C.3). To obtain the finite element equations, we calculate the load resultants at nodes $i = 1, 2$

$$\begin{aligned} Q_1 &= -Q_x(-L/2) \ , & Q_2 &= Q_x(L/2) \ , \\ M_1 &= M_x(-L/2) \ , & M_2 &= -M_x(L/2) \ . \end{aligned} \tag{C.4}$$

These equations can be written in the form

$$\mathbf{K}\mathbf{u} = \mathbf{f} \ , \tag{C.5}$$

where

$$\mathbf{u} = \{w_1 \quad \phi_1 \quad w_2 \quad \phi_2\}^{\mathrm{T}} \tag{C.6}$$

is the displacement vector,

$$\mathbf{f} = \{Q_1 \quad M_1 \quad Q_2 \quad M_2\}^{\mathrm{T}} \tag{C.7}$$

is the nodal force vector and the stiffness matrix reads

$$\mathbf{K} = \Delta \begin{bmatrix} 12 & 6L & -12 & 6L \\ 6L & 4\left(D_Q L^2 + 3D_{xx}\right)/D_Q & -6L & 2\left(D_Q L^2 - 6D_{xx}\right)/D_Q \\ -12 & -6L & 12 & -6L \\ 6L & 2\left(D_Q L^2 - 6D_{xx}\right)/D_Q & -6L & 4\left(D_Q L^2 + 3D_{xx}\right)/D_Q \end{bmatrix} \ , \tag{C.8}$$

where

$$\Delta = \frac{D_Q D_{xx}}{L(D_Q L^2 + 12D_{xx})} \ . \tag{C.9}$$

Acknowledgements

The authors acknowledge the Finland Distinguished Professor (FiDiPro) programme: "Nonlinear response of large, complex thin-walled structures" supported by Tekes (The Finnish Funding Agency for Technology and Innovation) and industrial partners Napa, SSAB, Deltamarin, Konetekнologiakeskus Turku and Meyer Turku.

References

[1] Yang F, Chong ACM, Lam DCC, Tong P. Couple stress based strain gradient theory for elasticity. Int J Solids Struct 2002;39(10):2731–43.

[2] Shaat M. Physical and mathematical representations of couple stress effects on micro/nanosolids. Int J App Mech 2015;7(1):1550012–1–28.

[3] Shaat M, Abdelkefi A. On a second-order rotation gradient theory for linear elastic continua. Int J Eng Sci 2016;100:74–98.

[4] Tiersten HF, Bleustein JL. Generalized elastic continua, In: Herrmann G. (Ed.), R. D. Mindlin and Applied Mechanics. New York: Pergamon Press; 1974.

[5] Lam DCC, Yang F, Chong ACM, Wang J, Tong P. Experiments and theory in strain gradient elasticity. J Mech Phys Solids 2003;51(8):1477–508.

[6] McFarland AW, Colton JS. Role of material microstructure in plate stiffness with relevance to microcantilever sensors. J Micromech Microeng 2005;15(5):1060–7.

[7] Park SK, Gao XL. Bernoulli–Euler beam model based on a modified couple stress theory. J Micromech Microeng 2006;16(11):2355–9.

[8] Kong S, Zhou S, Nie Z, Wang K. The size-dependent natural frequency of Bernoulli–Euler micro-beams. Int J Eng Sci 2008;46(5):427–37.

[9] Akgöz B, Civalek Ö. Strain gradient elasticity and modified couple stress models for buckling analysis of axially loaded micro-scaled beams. Int J Eng Sci 2011;49(11):1268–80.

[10] Xia W, Wang L, Yin L. Nonlinear non-classical microscale beams: static bending, postbuckling and free vibration. Int J Eng Sci 2010;48(12):2044–53.

[11] Abdi J, Koochi A, Kazemi AS, Abadyan M. Modeling the effects of size dependence and dispersion forces on the pull-in instability of electrostatic cantilever nems using modified couple stress theory. Smart Mater Struct 2011;20(5):055011–1–9.

[12] Rahaeifard M, Kahrobaiyan MH, Asghari M, Ahmadian MT. Static pull-in analysis of microcantilevers based on the modified couple stress theory. Sensor Actuat A-Phys 2011;171(2):370–4.

[13] Ma HM, Gao XL, Reddy JN. A microstructure-dependent Timoshenko beam model based on a modified couple stress theory. J Mech Phys Solids 2008;56(12):3379–91.

[14] Asghari M, Kahrobaiyan MH, Ahmadian MT. A nonlinear Timoshenko beam formulation based on the modified couple stress theory. Int J Eng Sci 2010;48(12):1749–61.

[15] Asghari M, Rahaeifard M, Kahrobaiyan MH, Ahmadian MT. The modified couple stress functionally graded Timoshenko beam formulation. Mater Design 2011;32(3):1435–43.

[16] Reddy JN. Microstructure-dependent couple stress theories of functionally graded beams. J Mech Phys Solids 2011;59(11):2382–99.

[17] Ke LL, Wang YS. Size effect on dynamic stability of functionally graded microbeams based on a modified couple stress theory. Compos Struct 2011;93(2):342–50.

[18] Ke LL, Wang YS, Yang J, Kitipornchai S. Nonlinear free vibration of size-dependent functionally graded microbeams. Int J Eng Sci 2012;50(1):256–67.

[19] Ansari R, Gholami R, Sahmani S. Free vibration analysis of size-dependent functionally graded microbeams based on the strain gradient Timoshenko beam theory. Compos Struct 2011;94(1):221–8.

[20] Roque CMC, Fidalgo DS, Ferreira AJM, Reddy JN. A study of a microstructure-dependent composite laminated Timoshenko beam using a modified couple stress theory and a meshless method. Compos Struct 2013;96:532–7.

[21] Ghayesh MH, Farokhi H, Amabili M. Nonlinear dynamics of a microscale beam based on the modified couple stress theory. Compos Part B-Eng 2013;50:318–24.

[22] Romanoff J, Reddy JN. Experimental validation of the modified couple stress Timoshenko beam theory for web-core sandwich panels. Compos Struct 2014;111:130–7.

[23] Romanoff J, Reddy JN, Jelovica J. Using non-local Timoshenko beam theories for prediction of micro-and macro-structural responses. Compos Struct 2015;.

[24] Arbind A, Reddy JN. Nonlinear analysis of functionally graded microstructure-dependent beams. Compos Struct 2013;98:272–81.

[25] Komijani M, Reddy JN, Eslami MR. Nonlinear analysis of microstructure-dependent functionally graded piezoelectric material actuators. J Mech Phys Solids 2014;63:214–27.

[26] Kahrobaiyan MH, Asghari M, Ahmadian MT. A Timoshenko beam element based on the modified couple stress theory. Int J Mech Sci 2014;79:75–83.

[27] Jeffrey A, Zwillinger D. Gradshteyn and Ryzhik's Table of Integrals, Series, and Products. New York: Academic Press; 2007.

[28] Karttunen AT, von Hertzen R. Exact theory for a linearly elastic interior beam. Int J Solids Struct 2016;78:125–30.
[29] Reddy JN, Wang CM, Lam KY. Unified finite elements based on the classical and shear deformation theories of beams and axisymmetric circular plates. Commun Numer Meth En 1997;13(6):495–510.